Journal of Materials Chemistry C

Accepted Manuscript

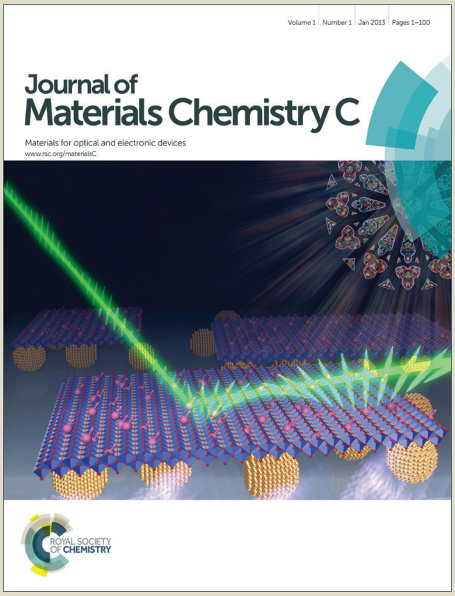

ROYAL SOCIETY OF CHEMISTRY

www.rsc.org/materialsC

A new strategy for achieving white-light-emission of lanthanide complexes: effective control of energy transfer from blue-emissive fluorophore to Eu(III) centres

Junqing Zhang, Hongfeng Li,* Peng Chen, Wenbin Sun, Ting Gao, Pengfei Yan*

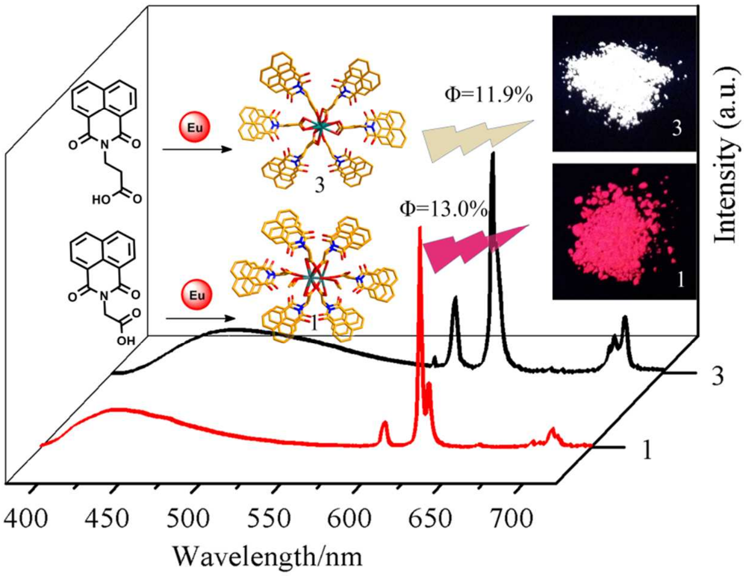

According to control energy transfer from the singlet state of blue-emitting fluorophore to Eu(III) ions, a white-light-emitting Eu(III) coordination polymers based on 1,8-naphthalimide derived ligand was synthesized, and three primary colours are well balanced by adjusting the length of linkers.

Journal Name RSCPublishing

ARTICLE

Cite this: DOI: 10.1039/x0xx00000x

Received 00th January 2012,
Accepted 00th January 2012

DOI: 10.1039/x0xx00000x

www.rsc.org/

A new strategy for achieving white-light-emission of lanthanide complexes: effective control of energy transfer from blue-emissive fluorophore to Eu(III) centres

Junqing Zhang, Hongfeng Li,* Peng Chen, Wenbin Sun, Ting Gao, Pengfei Yan*

Two novel bifunctional 1,8-naphthalimide-based ligands incorporating coordinated carboxyl group and blue emitting 1,8-naphthalimide, 2-(1,8-naphthalimido)ethanoic acid (HL^1) and 3-(1,8-naphthalimido)propanoic acid (HL^2), are designed for synthesis of white light emitting lanthanide complexes. Self-assembly of ligands with lanthanide ions formed two series of 1D coordination polymers $\{Ln(L^1)_3(CH_3OH)(H_2O)\}_n$ (Ln = Eu^{3+} (**1**), Gd^{3+} (**2**)) and $\{[Ln(L^2)_3(H_2O)]\cdot H_2O\}_n$ (Ln = Eu^{3+} (**3**), Gd^{3+}(**4**)). The single crystal X-ray crystallography analyses reveal the complexes feature 1D chain structure. In **1** and **3**, partial energy transfer from the 1,8-naphthalimide moieties to the metal centres results in sensitized Eu(III)-based emission in addition to the ligand-based blue/green luminescence. Through changing the length of the linkers between the chromophore and the metal centre, energy transfer efficiency of ligands-to-Eu is effectively controlled. In **1**, the emission spectrum is mainly dominated by the red light of the Eu(III) ions. However, the red light emission is suppressed in **3** due to the decrease of chromophore-to-Eu energy transfer efficiency. This effective adjustment realized the balance of three primary colours, and thus resulting in white light emission of **3**. This result opens up a new synthetic strategy for white light emitting materials.

Introduction

White light emitting materials have recently merited particular attention due to their broad applications in lighting sources, backlight and full-colour displays.[1] Generally, the realization of white light emission requires the generation and intensity control of the three fundamental red, green and blue (RGB) light emission in bulk materials. The trichromatic approach is the mostly employed for producing white-light materials. In the past decades, reported white-light-emitting materials contain nanocrystals,[2] quantum dots,[3] lanthanide-doped inorganic materials,[4] small organic molecules,[5] polymers,[6] and the lanthanide complexes.[7] Benefitting from high colour purity, high photoluminescence efficiency of lanthanide ions, and the exceptional tenability, structural diversity of coordination polymers (CPs), there has been great interest devoted to white-light emitting lanthanide-organic coordination polymers (Ln-CPs) in recent years.[8]

In Ln-CPs, white light emission is generally achieved by co-doping red-light-emitting Eu(III) and green-light-emitting Tb(III) ions into the corresponding blue-light-emitting isostructural Ln-CPs (Ln = La or Gd).[9] It is known as three component approach. Another similar doping approach for obtaining white light is known as two component approach, in which La or Gd-CPs emit blue-green light, whereas Eu(III) is as a only doping and emit red light.[10] Recently, a more simple method is employed that only a Sm(III) ion is involved in white light emitting framework.[11] It can be named as one-component approach. Compared with the multi-component approach, this way will considerably simplify the preparation of the white-light-emitting complexes.

It is notable that in these works mentioned above, the ligands not only play a role as sensitizer for the Ln(III) ions via an "antenna effect", but also as a blue-emitting source. In fact, blue emission of ligand considerably implies the less energy transfer from the ligand to the Ln(III) ions due to the mismatch of energy level between ligand and lanthanides. It is known to all that the widely accepted energy transfer pathway for the sensitization Ln(III) ions luminescence consists of excitation of the ligands into their excited singlet states, subsequently intersystem crossing to their triplet states, then the energy transfer from the triplet states to the excited states of the Ln(III) ions.[12] In order to make energy transfer effective, the energy-level match between the triple states of the ligand and the Ln(III) ions became one of the most important factors dominating the luminescence properties of the complexes. According to Latva's empirical rule,[13] an optimal ligand-to-metal energy transfer process for Eu(III) ions needs the energy gap ΔE ($^3\pi\pi^* - {}^5D_0$) > 2500 cm^{-1}. The lowest excited energy levels of Eu(III) ion is located at 17 500 cm^{-1} ($^5D_0$, 570 nm), which means the triple states of the ligand should be at least higher than 20 000 cm^{-1} (500 nm). According to Reinhoudt's empirical rule,[14] the intersystem crossing process becomes effective when ΔE ($^1\pi\pi^* - {}^3\pi\pi^*$) is at least 5000 cm^{-1}, thus the singlet states of the ligand should higher than 25 000 cm^{-1} (400 nm) for effectively sensitizing Eu(III) ions luminescence, that is, the emission bands of the ligand should be located in UV regions (< 400 nm). Therefore, ligand-based blue emission generally means the ligands have the lower single- and triple-states levels, and thus leading to energy-level mismatch between ligand and Eu(III) ions. This is the main reason why the luminescence quantum yields are relatively lower in the reported white light emission Ln-CPs. Therefore, an accurate design of ligand that make it not only emits blue light, but also as effective sensitizer, is crucial for achieving high efficiency white light emission.

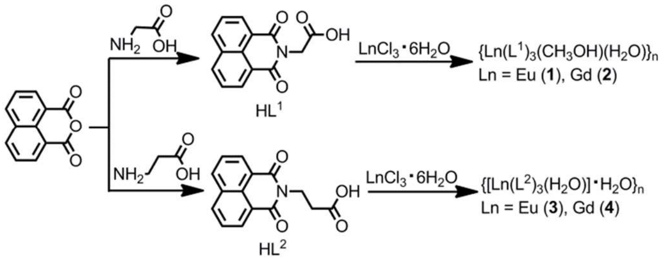

Scheme 1 Syntheses of the HL^1, HL^2 and their complexes.

We are interested in exploring novel white-light-emitting materials of lanthanide complexes.[15] Herein, two blue-emitting ligands HL^1 and HL^2 are designed for synthesis of white-light-emitting Ln-CPs (see Scheme 1). The ligands are composed of a coordinating carboxyl decorated with a methylene and an ethidene linkers fitted with a 1,8-naphthalimide at their extremity. As a fluorophore, 1,8-naphthalimide has widely used in fluorescence sensors, biological imaging, and lighting devices due to their high photostability, and high luminescence quantum yields.[16] In complexes, 1,8-naphthalimide do not directly coordinate to Ln(III) ions, but separated from Ln(III) centres by the σ-bonds of alkyl groups. This separation may result in the considerable decrease of intersystem crossing efficiency caused by the heavy atom effect of lanthanide ions; meanwhile increase the rate of energy transfer from the singlet excited level to the Ln(III) ions.[17] Therefore, the sensitization of the Eu(III) ion by the singlet state of 1,8-naphthalimide moiety in ligand should be possible. 1,8-naphthalimide emits blue fluorescence from the singlet π–π^* state with the emission bands range from 350 nm to 475 nm. Thus, the energy gap ΔE ($^1\pi\pi^* - {}^5D_0$) is in the range of 3071–3553 cm^{-1}, meeting the requirement of energy gap above 2500 cm^{-1}. In addition, aggregation of 1,8-naphthalimide units in solid state will result in a red-shifted and enhancement emission band.[18] Therefore, the 1,8-naphthalimide unit that combines the monomer blue- and aggregate blue/green-luminescence is suitable for the construction of Eu(III)-based white light materials. In this paper, we utilized the ligands HL^1, HL^2 and Eu(III) ions successfully to prepare two 1D chain coordination polymers **1** and **3**. Upon excited with UV, partial energy transfer from the ligands to metal centre results in Eu(III)-based red light emission in addition to the ligand-based blue/green emission. According to adjust the length of the linkers, energy transfer efficiency is effectively controlled, and white light emission is subsequently obtained in **3**. This open a new way for synthesis of lanthanide white light materials that Ln(III) ions luminescence is sensitized by the singlet excited state of blue-emitting fluorophore, meanwhile three primary colours are balanced by controlling ligands-to-Eu(III) energy transfer efficiency according to change the length of linkers. In addition, **3** will be the only example to achieve white light emission from the Ln-CPs that only one ligand and one lanthanide are present.

Experimental

Materials and Instruments

The commercially available chemicals were analytical reagent grade and used without further purification. 1,8-naphthalic anhydride (99%, A. R.) was purchased from Shanghai Darui Finechemical Co. (Shanghai, China). $LnCl_3·6H_2O$ was prepared according to the literature by dissolving 99.99% oxide in a slight excess of hydrochloric acid. The solution was evaporated and the precipitate was recrystallized from water. All other starting materials were of analytical grade as obtained from commercial sources without further purification.

Elemental analyses (C, H, N and O) were performed on an Elementar Vario EL cube analyser. FT-IR spectra were obtained on a Perkin-Elmer Spectrum One spectrophotometer by using KBr disks in the range of 4000–450 cm^{-1}. UV spectra were recorded on a Perkin-Elmer Lambda 25 spectrometer. Thermal analyses were conducted on a Perkin-Elmer STA 6000 with a heating rate of 10 ºC min^{-1} in a temperature range from 30 ºC to 800 ºC. Electrospray TOF (ESI-TOF) mass spectra were recorded on Bruker maXis mass spectrometers. Crystal data of the complexes were collected on a Xcalibur, Eos, Gemini diffractometer with Mo Kα radiation (λ = 0.71073 Å). All data were collected at a temperature of 23 ± 2 ºC. The structures were solved by the direct methods and refined on F2 by full-matrix least-squares using the SHELXTL-97 program. The Ln(III) ions were easily located and then non-hydrogen atoms (C, N and O) were placed from the subsequent Fourier-difference maps. All non-hydrogen atoms were refined anistropically. A summary for data collection and refinements were given in Table S1. Excitation and emission spectra were measured with an Edinburgh FLS 920 fluorescence spectrophotometer. Luminescence lifetimes were recorded on a single photon counting spectrometer from Edinburgh Instrument (FLS 920) with microsecond pulse lamp and a picosecond laser as the excitation sources. The data were analysed by software supplied by Edinburgh Instruments. The quantum yields for the complexes were determined at room temperature through an absolute method using an Edinburgh instruments' integrating sphere coupled to the modular Edinburgh FLS 920 fluorescence spectrophotometer. The values reported are the average of three independent determinations for each sample. The absolute quantum yield was calculated using the following expression:

$$\Phi = \frac{\int L_{emission}}{\int E_{reference} - \int E_{sample}} \qquad (1)$$

Where $L_{emission}$ is the emission spectrum of the sample, collected using the sphere, E_{sample} is the spectrum of the incidence light used to excite the sample, collected using the sphere, $E_{reference}$ is the spectrum of the light used for excitation with only the reference in the sphere. The method is accurate within 10%. The Commission International de I'Eclairage (CIE) colour coordinates were calculated on the basis of the international CIE standards.[19]

Synthesis of 2-(1,8-naphthalimido)ethanoic acid (HL^1). A mixture of glycine (6.01 g, 0.08 mol) and triethylamine (8.08 g, 0.08 mol) in 170 mL *i*-propanol was stirred for 10 minutes at room temperature, followed by the addition of 1,8-naphthalic anhydride (7.93 g, 0.04 mol) in portions, which was then refluxed for 5 hours. After cooled to the room temperature, the resulting mixture was poured into 500 mL ice water and acidified to pH = 5–6 using hydrochloric acid (2 M solution). The resulting white precipitate was filtered and washed with water three times. Recrystallization from THF and water gave white crystals (7.45 g, 73% yield). Anal. Calc. for $C_{14}H_9NO_4$ (255.23): C, 65.88; H, 3.55; N, 5.49; O, 25.07. Found: C, 65.97; H, 3.50; N, 5.44; O, 25.09. ^1H NMR (DMSO-d_6, 400Mz): δ (*ppm*): 13.05 (s, 1H), 8.54 (t, *J* = 7.10 Hz, 4H), 7.93 (d, *J* = 8.06 Hz, 2H), 4.76 (s, 2H); IR (KBr, cm^{-1}): 3336, 3016, 1705, 1663, 1590, 1432, 1380, 1294, 1257, 1238, 977, 781. ESI-MS m/z 256 $[M + H]^+$.

Synthesis of 3-(1,8-naphthalimido)propanoic acid (HL^2). HL^2 was prepared in the same manner as used in HL^1. (7.64 g, Yield: 71%). Anal. Calc. for $C_{15}H_{11}NO_4$ (269.25): C, 66.91; H, 4.12; N, 5.20; O, 23.77. Found: C, 66.88; H, 4.21; N, 5.23; O, 23.68. ^1H NMR (DMSO-d_6, 400Mz): δ (*ppm*): 12.32 (s, 1H), 8.52–8.46 (m, *J* = 6.26 Hz, 4H), 7.91–7.87 (m, *J* = 7.41 Hz, 2H), 4.31–4.27 (t, *J* = 7.65 Hz, 2H), 2.63–2.60 (t, *J* = 7.81 Hz, 2H); IR (KBr, cm^{-1}): 3362, 1700, 1658, 1588, 1550, 1434, 1382, 1345, 1233, 1032, 778. ESI-MS m/z 270 $[M + H]^+$, 292 $[M + Na]^+$.

Synthesis of the complexes $\{Ln(L^1)_3(CH_3OH)(H_2O)\}_n$ [Ln = Eu (1), Gd(2)]. A methanol solution (10 mL) of HL^1 (15.3 mg, 0.06 mmol) and triethylamine (6.06 mg, 0.06 mmol) were allowed to diffuse slowly into the aqueous solution (10 mL) of $LnCl_3 \cdot 6H_2O$ (0.02 mmol) in a long test tube with a buffer layer of pure methanol placed between the two solutions. The tube was sealed and allowed to stand at room temperature. Colourless crystals of **1** suitable for X-ray analysis were obtained in about two weeks.

$\{Eu(L^1)_3(CH_3OH)(H_2O)\}_n$ (1) Yield: 68%. Anal. Calc. for $C_{43}H_{30}N_3O_{14}Eu$: C, 53.54; H, 3.13; N, 4.36; O, 23.22. Found: C, 53.53; H, 3.19; N, 4.23; O, 23.24. IR (KBr, cm^{-1}): 3536, 3326, 3015, 1705, 1656, 1576, 1432, 1380, 1298, 1238, 977, 781.

$\{Gd(L^1)_3(CH_3OH)(H_2O)\}_n$ (2) Yield: 65%. Anal. Calc. for $C_{43}H_{30}N_3O_{14}Gd$: C, 53.25; H, 3.12; N, 4.33; O, 23.09. Found: C, 53.23; H, 3.18; N, 4.28; O, 23.12. IR (KBr, cm^{-1}): 3327, 3078, 1705, 1663, 1570, 1435, 1380, 1293, 1237, 977, 781.

Synthesis of the complexes $\{[Ln(L^2)_3(H_2O)]\cdot H_2O\}_n$ [Ln = Eu (3), Gd (4)]. The methods used for the syntheses of complexes **3** and **4** are similar to that used for **1** and **2**, except HL^1 is replaced by HL^2.

$\{[Eu(L^2)_3(H_2O)]\cdot H_2O\}_n$ (3) Yield: 67%. Anal. Calc. for $C_{45}H_{34}N_3O_{14}Eu$: C, 55.44; H, 3.45; N, 4.23; O, 22.56. Found: C, 55.42; H, 3.46; N, 4.20; O, 22.59. IR (KBr, cm^{-1}): 2917, 2638, 1693, 1653, 1585, 1438, 1352, 1271, 1221, 1173, 929, 781.

$\{[Gd(L^2)_3(H_2O)]\cdot H_2O\}_n$ (4) Yield: 63%. Anal. Calc. for $C_{45}H_{34}N_3O_{14}Gd$: C, 54.16; H, 3.43; N, 4.21; O, 22.44. Found: C, 54.20; H, 3.46; N, 4.20; O, 22.48. IR (KBr, cm^{-1}): 3536, 3326, 3015, 1702, 1661, 1625, 1591, 1563, 1532, 1441, 1384, 1345, 1263, 1235, 1033, 780.

Result and discussion

Characterization of the ligands and complexes

The synthetic procedures adopted for the ligands HL^1, HL^2 and their Ln(III) complexes **1**–**4** are described in Schemes 1. The ^1H NMR spectra of HL^1 and HL^2 obtained at 400 MHz in DMSO-d_6 are shown in Fig. S1 and S2 (ESI†). The chemical shift values of aromatic protons are in the range of 7.87–7.95 and 8.46–8.56 ppm, respectively. The chemical shift values in HL^1 are slightly bigger than that in HL^2 due to the stronger deshielding effect of the withdrawing carboxyl group in HL^1, which is more close to the aromatic protons than in HL^2. In HL^1, the singlet peaks present at 13.05 and 4.75 ppm are attributed to the carboxylate proton and methylene protons, respectively. In HL^2, the carboxylate proton presents at 12.32 ppm. Two sets of triplet peaks observed at 2.60–2.63 and 4.27–4.31 ppm are attributed to the ethidene protons Hb' and Hc', respectively. The triplets are the results of the spin-spin coupling of the adjacent protons, and being close to the withdrawing carboxyl group make the Hb' presents at downfield. The FT–IR spectra of complexes **1**–**4** show a broad absorption in the region of 3000–3500 cm^{-1}, thereby indicating the presence of solvent molecules in the complexes. The carbonyl stretching frequency of imide in free ligands ($\nu_{s\ (C=O)}$ = 1656 cm^{-1}) almost do not shift in **1**–**4**, which means the absence of coordination of these imide groups to the Ln(III) cations. However, the stretching vibrations of the carboxyl groups in free ligands ($v_{s\ (C=O)}$ = 1702 cm^{-1}) shift to lower wavenumbers in the complexes (**1**, 1569 cm^{-1}; **2**, 1567 cm^{-1}; **3**, 1546 cm^{-1} and **4**, 1532 cm^{-1}), thus indicating the coordination of the oxygen atoms to the lanthanide ions. To examine the thermal stability and solvent content of the complexes, thermogravimetric analyses are carried out for **1**–**4** (Fig. S3†). The TG curves of **1**–**2** are similar and exhibit two main weight losses. The first step of weight loss occurs between 150 and 230 ℃ (**1**, found: 5.1%, calcd: 5.2%; **2**, found: 5.1 %, calcd: 5.2%), corresponding to the losses of water and methanol molecules. The second step from 360 to 495 ℃ corresponds to the thermal decomposition of the organic ligands and finally leading to the formation of the stoichiometric amounts of Ln_2O_3 (**1**, found: 18.4%, calcd: 18.2%; **2**, 18.6%, calcd: 18.7%). Similarly, complexes **3** and **4** all undergo mass loss of about 3.5% between 60 to 150 ℃, corresponding to the loss of two molecule of water (calcd: 3.6% for **3** and **4**). Then, a long plateau is observed until a full decomposition at *ca*. 300 ℃.

Structural description

Structural analysis of {Eu(L^1)$_3$(CH$_3$OH)(H$_2$O)}$_n$ (1). The single crystal X-ray analysis reveals that **1** crystallize in the monoclinic space group *C2/c* (Table S1). The structure unit [Eu(L^1)$_3$(CH$_3$OH)(H$_2$O)] of **1** consists one crystallographically independent Eu(III) ion, three L^1 ligands, one coordinated water and one coordinated methanol molecule.

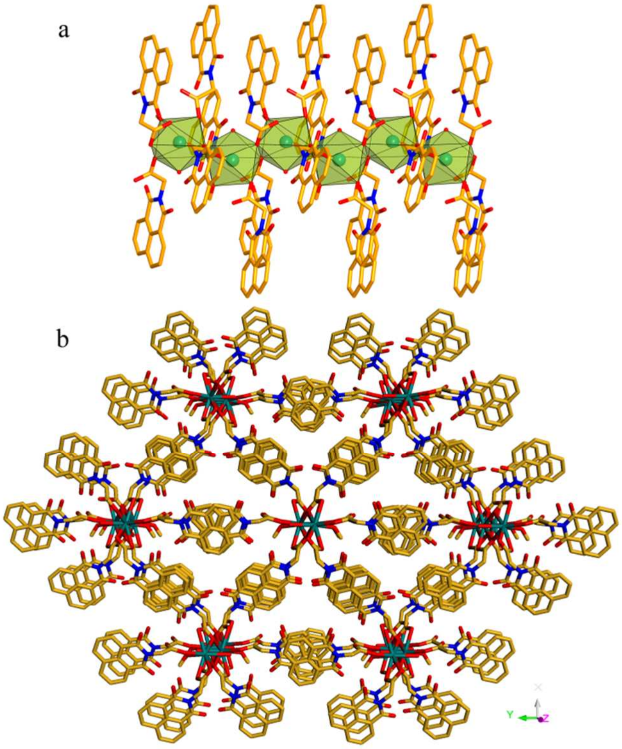

Fig. 1 View of the structure of 1: (a) Stick depiction of infinite 1D Eu chain. (b) 3D structure of **1** along the [0 0 1] direction. All H atoms are omitted for clarity.

The Eu(III) centre is coordinated with seven oxygen atoms from five L^1 ligands, one hydrate oxygen atom and one methanol oxygen atom. The Eu–O bond distances are in range of 2.391(4)–2.551(3) Å. One L^1 ligand and one ethanol molecule are found disordered and their occupancy is treated as 0.5:0.5. The carboxylate groups of L^1 ligand adopt two different types of coordination modes: (i) one of the carboxylate group adopts monodentate coordination mode (Fig. S4); (ii) the other one adopts a μ$_2$-ŋ^1-ŋ^2-bridging coordination mode (one oxygen atom of the carboxylate group connects two Eu atoms, the other one connects one europium atom and the carboxylate group coordinates to two metal atoms). Eu(III) and L^1 are connected to form a 1D chain structure (Fig. 1a), which are stitched together to form a 3D framework via parallel π–π interactions between naphthalimide moieties among six neighbouring chains (Fig. 1b). The π–π distances are 3.550 and 3.414 Å, respectively (Fig. S6).

Structure analysis of {[Eu(L^2)$_3$(H$_2$O)]·H$_2$O}$_n$ (3). The single crystal X-ray diffraction analysis reveals that **3** crystallize in the monoclinic space group *P*2$_1$/*c* (Table S1). The structure unit [Eu(L^2)$_3$(H$_2$O)]·H$_2$O of **3** contains one Eu(III) ion, three L^2 ligands, one coordinated water molecule and one lattice water molecule.

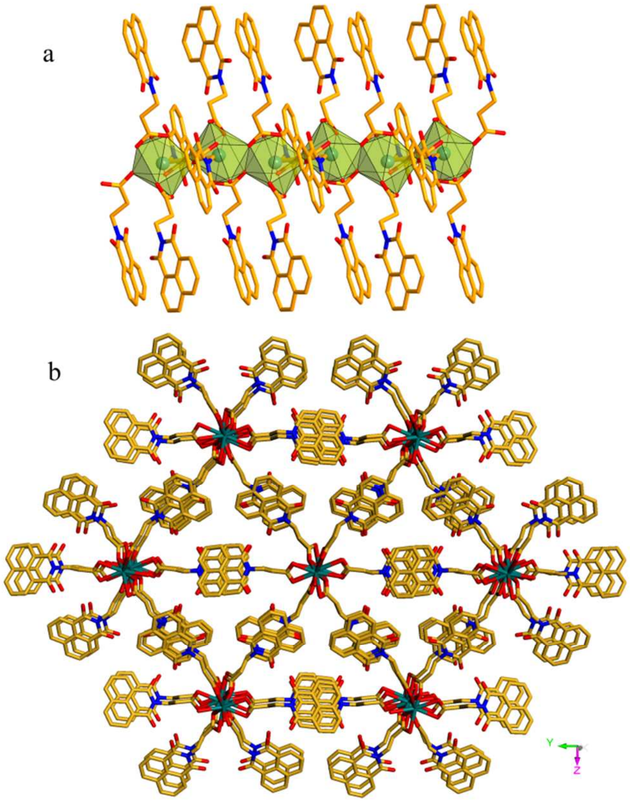

Fig. 2 View of the structure of **3**: (a) Stick depiction of infinite 1D Eu chain. (b) 3D structure of **3** along the [1 0 0] direction. All H atoms are omitted for clarity.

The Eu(III) centre is coordinated with eight oxygen atoms from five L^2 ligands and one hydrate oxygen atom. The Eu–O bond distances are in range of 2.335(9)–2.544(9) Å. In contrast to the coordination fashion in **1,** the carboxylate group in **3** adopt another two different types of coordination modes: (i) μ_1-η^1-η^1-bridging fashion; (ii) μ_1-η^1-η^2-bridging fashion, (Fig. S5). As observed in **1**, Eu(III) and L^2 are further connected to form a one-dimensional chain structure in **3** (Fig. 2a), which are stitched together to form a 3D framework via parallel π–π interactions between naphthalimide moieties among six neighbouring chains (Fig. 2b). The π–π distances are 3.454 and 3.816 Å, respectively (Fig. S7). As the length of the alkyl chain is increased, the configuration of the 1,8-naphthalimide moieties in **3** present some alternations in comparison to that in **1**. And longer distances are detected between the adjacent chains, resulting in larger space for the full accommodation of naphthalimide groups. The adjacent Eu···Eu distances in the same strand is 4.200 Å for **1** and 4.095 Å for **3**. And the $Eu\cdots N_{amide}$ distances in the range of 6.401–6.645 Å in **3** are relatively longer than that of 5.108–5.874 Å in **1** with the increase of the alkyl chain length. The powder XRD patterns of the complexes **1**, **2** and **3**, **4,** as shown in Fig. S8, coincide with the calculated PXRD pattern of their corresponding structures, indicating that the Gd complexes are isostructural with their corresponding Eu analogues.

The photophysical properties of the ligands

The UV-Vis absorption spectra of the ligands HL^1 and HL^2 in methanol are shown in Fig. 3. The spectra display intense bands in the UV region at 250–370 nm with the maximum at 332 nm corresponding to the singlet-singlet $^1\pi$–π^* electronic transition of the 1,8-naphthalimide moieties in ligands. Similar spectra can also be observed in unsubstituted 1,8-naphthalimide.[20] Upon excitation with their maxima absorption bands, both ligands emit broad bands in the range of 330–525 nm with maxima around 386 nm in methanol. However, the emission bands of the ligands in solid state appear obvious red shift with the more broad bands in the range of 380–600 nm, which almost cover the whole blue-green regions of the spectra. The large red-shift of the emissive bands is the result of aggregation of ligands in the solid-state. Therefore, the ligands with the blue-green luminescence that combine the Eu(III) ions red luminescence are suitable for the construction of lanthanide white light materials.

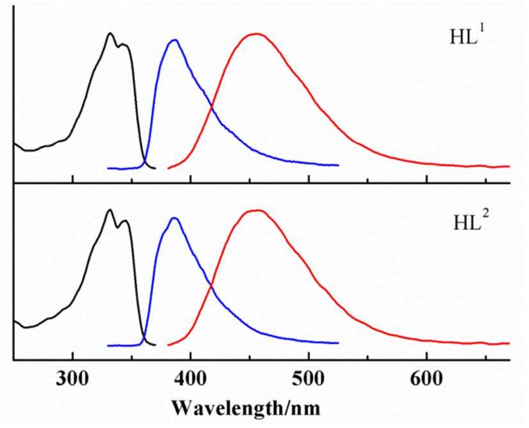

Fig. 3 Normalized absorption spectra of the ligands HL^1 and HL^2 (blank lines); emission spectra (blue lines) in CH_3OH; emission spectrum in solid state (red lines).

Luminescence properties of the complexes

As mentioned above, the ligands emit blue-green fluorescence in the solid state. Therefore, it is possible to achieve white light emission for Eu(III) complexes by incorporating the ligand-based blue-green emission and Eu(III) ions red emission. For investigating the photophysical properties of the ligands in complexes and the process of energy transfer from ligand to the metal centres, two Gd(III) complexes $\{Gd(L^1)_3(CH_3OH)(H_2O)\}_n$ (**2**) and $\{[Gd(L^2)_3(H_2O)]\cdot H_2O\}_n$ (**4**) are prepared. Because the Gd(III) ions has no energy levels below 32 150 cm^{-1}, and thus cannot accept energy from the triplet and singlet sates of the ligands. The complexes **2** and **4** could therefore be used as models to study the fluorescence of the ligands in complexes.

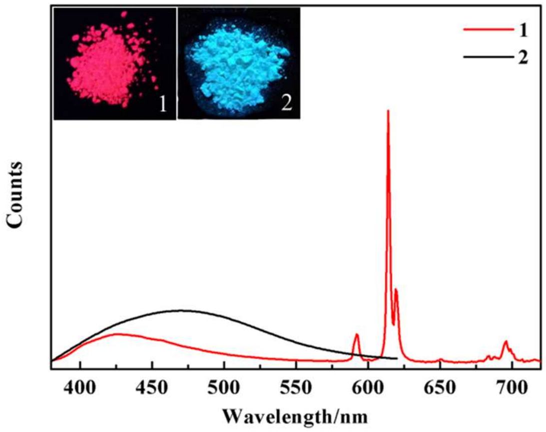

Fig. 4 Emission spectra of the complexes **1** and **2** in the solid state

As shown in Fig. 4, the complexes **1** and **2** all show characteristic blue-green emissions of the ligand HL^1 with the bands in the range of 375–600 nm. In comparison with the emission of the ligand in complex **2**, the emissive intensity of the ligand in **1** shows obvious decrease, and the maximum of the emission band blue-shifts from 475 nm to 420 nm. Moreover, **1** also shows a series of characteristic narrow band emissions of Eu(III) ions at 590, 614, 650, and 696 nm, corresponding to the $^5D_0 \rightarrow {}^7F_J$ (J = 1, 2, 3, 4) transition. It indicates the appearance of partial energy transfer from the ligand to Eu(III) ions. It is worth noting that the intensity of the low-energy fluorescence band of the ligand in **1** decrease obviously compared to that observed in **2**, which means the energy in this region better match the $^5D_0$ level of Eu(III) ion. However, it is a pity that the efficient energy transfer from the ligand to Eu(III) ions results in small ratio of blue-to-red emission components, and the complex **1** still emits red light dominated by the characteristic emission bands of Eu(III) ions. Upon excited at 320 nm, its CIE coordinate is located at (0.403, 0.164). In view of the possible effect of the excited wavelengths on emissive components of the complex, we investigated the variation trends of the emission spectra with the excitation wavelengths changing from 300 to 380 nm (Fig. S9). The corresponding emission colours are illustrated in the CIE chromaticity diagram, while the corresponding CIE colour coordinates are listed in Table S2. It can be seen that the colour coordinates are almost constants and the emission colours located at red region of chromaticity diagram.

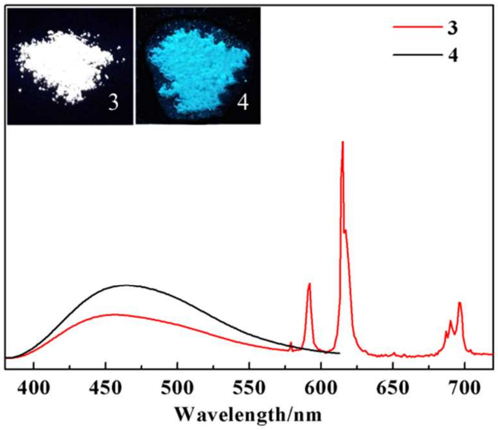

Fig. 5 Emission spectra of the complexes **3** and **4** in the solid state

In order to make the complex a better white-light emitter, it should be necessary to decrease the efficiency of ligand to Eu(III) energy transfer process such that the ratio of blue-to-red emission components is increased to give a better balance. Herein, we synthesized HL^2 to adjust the distance between the chromophore and the carboxylic group to reduce the energy transfer efficiency. The emission spectra of **3** and **4** are shown in Figure 5. Upon excited at 320 nm, the complexes again show ligand-based blue-green emission as that observed in **1** and **2**. Similarly, the relative emission intensity of ligand in **3** also shows obviously decrease in comparison to that in **4**. In addition, a series of characteristic emission bands of Eu(III) ions are also observed in complex **3**. Fortunately, the complex **3** displays bright white light to the eyes under UV irradiation. As excitation at 320 nm, **3** exhibited a nearly white light emission with CIE coordinates of (0.338, 0.312), which is much closed to the standard white light (0.333, 0.333) according to the 1931 CIE diagram. Furthermore, the variation trends of the emission spectra for **3** with the excitation wavelengths are shown in Fig. S10. Notably, all the CIE colour coordinates are almost constant and the colours of emissions fall within the white region of the 1931 CIE chromaticity diagram.

In addition to the steady-state emission, we also carried out the luminescence quantum yields and the time-resolved photoluminescence decay dynamics study. The calculation results are listed in Table 1. The luminescence quantum yield of **1** measured under excitation at 320 nm reaches to a value of 13.0%. However, the value are comprised of two part emissions of the ligands and Eu(III) ions, in which the quantum yield of the ligand is 7.8%, and Eu(III) ion is 5.2%. In complex **3**, the luminescence quantum yield decrease up to 11.9% with the values of 8.1% for ligand and 3.8% for Eu(III) ions. Noteworthily, the value is higher than the most of reported white-light organic-metal materials.[8a, 10a, 21] In comparison to the ligand-centred quantum yields of the Eu(III) complexes, the corresponding Gd(III) complexes have higher values (16.5%, **2**; 14.8%, **4**). In order to investigate the effect of the length of linkers on the emission components of the complexes, the efficiency of the energy transfer from ligand to Eu(III) ions is estimated by

$$\Phi_{\mathrm{ET}} = 1-(\Phi_{\mathrm{ET}}^{\mathrm{Eu}} / \Phi_{\mathrm{ET}}^{\mathrm{Gd}}) \qquad (2)$$

Where $\Phi_{\mathrm{ET}}^{\mathrm{Eu}}$ is the quantum yield of the residual energy transfer emission of the ligand in the Eu complexes and $\Phi_{\mathrm{ET}}^{\mathrm{Gd}}$ is the ligand-centred quantum yields of the non-emissive Gd complexes in the absence of any energy transfer to the metal. According to this equation, the calculated value for **1** (Φ_{ET} = 52.7%) is higher than that for **3** (Φ_{ET} = 45.2%). It indicates that the increase of the length of the linkers between the chromophore and the metal centre effectively decrease ligand-to-metal energy transfer efficiency, and thus balance the RGB luminescence components in **3**.

Table 1 Summary of quantum yields (Φ) and lifetimes (τ) of complexes **1**–**4**.

Parameters	1	2	3	4
$L\tau_{obs}$ (ns)	1.14 5.40	4.47 13.67	3.13 11.09	6.17 18.89
$Eu^{3+}\tau_{obs}$ (μs)	346	-	274	-
$QY_{(L)}$ (%)	7.8	16.5	8.1	14.8
$QY_{(Eu^{3+})}$ (%)	5.2	-	3.8	-
$QY_{overall}$ (%)	13.0	16.5	11.9	14.8

The luminescence lifetimes of the ligands in complexes **1**–**4** are determined by monitoring the emission decay curves of the ligands at 460 nm. Typical decay profiles are shown in Fig. S11, and all the decay curves are well-fitted by double-exponential functions. The relatively shorter lifetimes are at 1.14–6.17 ns, while the longer are at 5.40–18.89 ns. It is noted the lifetimes of the ligands in Eu(III) complexes are obviously shorter than that observed in corresponding Gd(III) complexes. It indicates the presence of a depopulation of the singlet states of ligands by energy transfer from ligand to Eu(III) ions. The luminescence lifetimes of Eu(III) ions are determined by monitoring the emission decay curves within the $^5D_0 \rightarrow {}^7F_2$ transition at 614 nm (Fig. S12). The decay curves give satisfactory fits to the single-exponential lifetimes, which suggest that only one species exists in the excited state in the two complexes. The values are 346 μs and 274 μs for **1** and **3**, respectively.

Energy transfer between ligands and Eu(III) ions

In general, energy transfer in the sensitized luminescence of Ln(III) ions is widely accepted to take place mainly from the triplet state of the sensitizer. Therefore, most research towards luminescent lanthanide complexes mainly focus on the design of the ligands with a triplet state matching the excited state energy level of lanthanide ions. Although seldom observed, energy transfer from the singlet state of the ligand to the metal centre has been evidenced in the recent examples.[22] It has been proven that when the intersystem crossing rate is smaller than about 10^{11} s^{-1}, a singlet transfer mechanism is consistent with the experimental data. In this paper, 1,8-naphthalimide unit as a sensitizer does not directly coordinate to Ln(III) ions, but be excluded from the first coordination sphere. This separation will obviously lower the intersystem crossing rate, meanwhile, improve the energy transfer rate from the singlet state to metal centres. The Gd(III) ions has no energy levels below 32 150 cm^{-1}, and thus cannot accept energy from the triplet and singlet sates of the ligands. Therefore, the emissions of the Gd complexes **2** and **4** undoubtedly originate from the singlet state transition of ligand in the absence of any energy transfer to Gd ions. As mentioned in the previous section, the luminescence quantum yields and lifetimes of the 1,8-naphthalimide moieties in **1** and **3** are obviously lower than the corresponding Gd(III) complexes **2** and **4**. In view of the same heavy atom effect of Eu(III) and Gd(III) ions on the intersystem crossing, thus the decrease of the luminescence quantum yields in Eu(III) complexes compared with the Gd(III) complexes can only be attributed to a direct energy transfer from the singlet state to the Eu(III) ions.

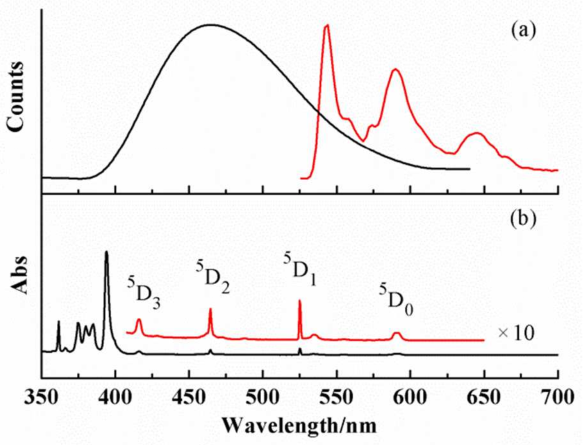

Fig. 6 (a) Emission spectrum of **4** at room temperature in the solid state (black line) and phosphorescence spectrum of HL^2 recorded at 77 K (red line). (b) UV-Vis absorption spectrum of $EuCl_3$ in water.

In addition, for a fast energy transfer, the ligands excited states and the accepting lanthanide energy level should be matched, that is, there should be spectral overlap between the donor (sensitizer) and the accepter (lanthanide ions) energy levels. The good match between the fluorescence profile of the 1,8-naphthalimide unit of Gd(III) complexes **2**, **4** and the highest density of f–f absorptions in the UV-Vis spectrum of Eu(III) in water (300–600 nm region) is shown in Fig. 6 and Fig. S13. The fluorescence from the naphthalimide unit which lies in the 375–600 nm regions almost overlaps with all the excited states of Eu(III) in the region from $^5D_0$ to $^5D_4$. Direct population of many of these from the $^7F_0$ ground state is allowed according to the selection rules for either Förster or Dexter energy-transfer to lanthanide ions.[23] In contrast the lower-energy phosphorescence of the naphthalimide unit occurs in an energy region where there is very little overlap with f–f absorptions of Eu(III), with the only overlapping f–f excited state being $^5D_0$. The poor donor and acceptor overlap, make T_1 → Eu ($^5D_0$) energy-transfer particularly slow. Moreover, direct population of the $^5D_0$ level from the $^7F_0$ ground state is forbidden by either Förster or Dexter energy-transfer, as it is a $J = 0 \rightarrow J = 0$ transition. Overall it is reasonable that naphthalimide (S_1) → Eu ($^5D_0$) energy-transfer should be much faster than $T_1 \rightarrow {}^5D_0$ energy transfer. This is different from the usually situation as observed in white-light-emitting lanthanide complexes where sensitization of lanthanide luminescence occurs exclusively from ligands T_1 states. In a word, sensitization of Eu(III) ions luminescence with the singlet excited state of the blue-emitting fluorescence should well solve the problem of the lower quantum yields of the white-light-emitting lanthanide complexes caused by the mismatch of energy levels between chromophore and Ln(III) ions.

Conclusion

In summary, we have successfully designed and synthesized a new coordination polymer $\{[Eu(L^2)_3(H_2O)]\cdot H_2O\}_n$ to achieve white light emission. Through adjusting the length of the linkers between the chromophore and the metal centre, energy transfer efficiency from ligands to Eu(III) ions is effectively controlled. This effective adjustment realized the balance of three primary colours, and thus resulting in white light emission of **3**. The luminescence quantum yield of **3** reaches up to 11.9%, higher than the most of reported white-light lanthanide complexes. This work realized the idea of construction of white light emitting materials by employing the blue-emitting fluorophore with high quantum yields as sensitizer for Eu(III) luminescence. Our future research will focus on exploiting similar Eu(III)-based white light materials with high quantum yields by employing the high efficiency blue-emitting fluorophore as ligands.

Acknowledgements

This work is financially supported by the National Natural Science Foundation of China (Nos. 51302068 & 21272061).

Notes and references

Key Laboratory of Functional Inorganic Material Chemistry (Heilongjiang University), Ministry of Education, School of Chemistry and Materials Science, Heilongjiang University, Harbin 150080, PR China. Fax: 86-451-86608042 E-mail: lhf4612@163.com; yanpf@vip.sina.com

Electronic Supplementary Information (ESI) available: ^{1}H NMR spectra of ligands, TG patterns, PXRD patterns, crystal data and structure refinement, CIE chromaticity coordinates diagrams of **1** and **3**, luminescence decay curves. CCDC 1031890–1031891 for **1** and **3**. For ESI and crystallographic data in CIF or other electronic format see DOI: 10.1039/b000000x/

1 (a) X. L. Yang, G. J. Zhou and W. Y. Wong, *J. Mater. Chem. C*, 2014, **2**, 1760–1778; (b) S. H. Kim, S. Park, J. E. Kwon and S. Y. Park, *Adv. Funct. Mater.*, 2011, **21**, 644–651; (c) J.-C. G. Bünzli, *Chem. Rev.*, 2010, **110**, 2729–2755; (d) C. D. Müller, A. Falcou, N. Reckefuss, M. Rojahn, V. Wiederhirn, P. Rudati, H. Frohne, O. Nuyken, H. Becker and K. Meerholz, *Nature*, 2003, **421**, 829–833; (e) K. T. Kamtekar, A. P. Monkman and M. R. Bryce, *Adv. Mater.*, 2010, **22**, 572–582; (f) B.-H. Kwon, H. S. Jang, H. S. Yoo, S. W. Kim, D. S. Kang, S. Maeng, D. S. Jang, H. Kim and D. Y. Jeon, *J. Mater. Chem.*, 2011, **21**, 12812–12818; (g) D. F. Sava, L. E. S. Rohwer, M. A. Rodriguez and T. M. Nenoff, *J. Am. Chem. Soc.*, 2012, **134**, 3983–3386.

2 (a) T. Wang, V. Chirmanov, W. H. M. Chiu and P. V. Radovanovic, *J. Am. Chem. Soc.*, 2013, **135**, 14520–14523; (b) M. M. Krause, J. Mooney and P. Kambhampati, *ACS Nano*, 2013, **7**, 5922–5929; (c) M. J. Bowers, J. R. McBride, S. J. Rosenthal, *J. Am. Chem. Soc.*, 2005, **127**, 15378–15379.

3 (a) C. L. Wang, S. H. Xu, Y. B. Wang, Z. Y. Wang and Y. P. Cui, *J. Mater. Chem. C*, 2014, **2**, 660–669; (b) N. S. Singh, N. K. Sahu and D. Bahadur, *J. Mater. Chem. C*, 2014, **2**, 548–555; (c) Q. Ju, D. Tu, Y. Liu, R. Li, H. Zhu, J. Chen, Z. Chen, M. Huang, X. Chen, *J. Am. Chem. Soc.*, 2012, **134**, 1323–1330.

4 (a) Z. Mao, D. Wang, Q. Lu, W. Yu and Z. Yuan, *Chem. Commun.*, 2009, 346–348; (b)P. V. Ramakrishna, D. B. R. K. Murthy and D. L. Sastry, *Spectrochim. Acta Part A*, 2014, **125**, 234–238.

5 (a) N. Nagarajan, G. Velmurugan, A. Prakash, N. Shakti, M. Katiyar, P. Venuvanalingam and R. Renganathan, *Chem. Asian J.*, 2014, **9**, 294–304; (b) K. Sakai, T. Ishikawa, T. Akutagawa, *J. Mater. Chem. C*, 2013, **1**, 7866–7871; (c) E. L. Williams, K. Haavisto, J. Li and G. E. Jabbour, *Adv. Mater.*, 2007, **19**, 197–202.

6 (a) H. B. Wu, G. J. Zhou, J. H. Zou, C.-L. Ho, W.-Y. Wong, W. Yang, J. B. Peng and Y. Cao, *Adv. Mater.*, 2009, **21**, 4181–4184; (b) J. Luo, X. Li, Q. Hou, Q. Peng, W. Yang and Y. Cao, *Adv. Mater.*, 2007, **19**, 1113–11170.

7 (a) X. Ma, X. Li, Y. E. Cha and L. P. Jin, *Cryst. Growth Des.*, 2012, **12**, 5227−5232; (b) G. J. He, D. Guo, C. He, X. L. Zhang, X. W. Zhao and C. Y. Duan, *Angew. Chem. Int. Ed.*, 2009, **48**, 6132–6135; (c) Q. Tang, S. X. Liu, Y. W. Liu, D. F. He, J. Miao, X. Q. Wang, Y. J. Ji and Z. P. Zheng, *Inorg. Chem.*, 2014, **53**, 289−293; (d) J. Cuan and B. Yan, *RSC Adv.*, 2013, **3**, 20077–20084; (e) A. Balamurugan, M. L. P. Reddy and M. Jayakannan, *J. Phys. Chem. B*, 2009, **113**, 14128–14138; (f) R. Shunmugam and G. N. Tew, *Polym. Adv. Technol.*, 2008, **19**, 596–601.

8 (a) Z. F. Liu, M. F. Wu, S. H. Wang, F. K. Zheng, G. E. Wang, J. Chen, Y. Xiao, A. Q. Wu, G. C. Guo and J. S. Huang, *J. Mater. Chem. C.*, 2013, **1**, 4634–4639; (b) M. L. Ma, J. H. Qin, C. Ji, H. Xu, R. Wang, B. J. Li, S. Q. Zang and S. R. Batten, *J. Mater. Chem. C*, 2014, **2**, 1085–1093; (c) S. Dang, J. H. Zhang and Z. M. Sun, *J. Mater. Chem.*, 2012, **22**, 8868–8873; (d) M. Zhu, Z. M. Hao, X. Z. Song, X. Meng, S. N. Zhao, S. Y. Song and H. J. Zhang, *Chem. Commun.*, 2014, **50**, 1912−1914. (e) A. R. Ramya, S. Varughese and M. L. P. Reddy, *Dalton Trans.*, 2014, **43**, 10940–10946.

9 (a) X. T. Rao, Q. Huang, X. L. Yang, Y. J. Cui, Y. Yang, C. D. Wu, B. L. Chen and G. D. Qian, *J. Mater. Chem.*, 2012, **22**, 3210–3214; (b) H. B. Zhang, X. C. Shan, L. J. Zhou, P. Lin, R. F. Li, E. Ma, X. G. Guo and S. W. Du , *J. Mater. Chem. C*, 2013, **1**, 888–891; (c) M. L. Ma, C. Ji and S. Q. Zang, *Dalton Trans.*, 2013, **42**, 10579–10586;

10 (a) S. Song, X. Li and Y. H. Zhang, *Dalton Trans.*, 2013, **42**, 10409–10412; (b) Y. Q. Wei, Q. H. Li, R. J. Sa and K. C. Wu, *Chem. Commun.*, 2014, **50**, 1820–1823.

11 Y. H. Zhang, X. Li and S. Song, *Chem. Commun.*, 2013, **49**, 10397–10399.

12 G. A. Crosby, R. M. Alire and R. E. Whan, *J. Chem. Phys.*, 1961, **34**, 743–748.

13 M. Latva, H. Takalo, V. M. Mukkala, C. Matachescu, J. C. Rodriguez-Ubis and J. Kankare, *J. Lumin.*, 1997, **75**, 149–169.

14 F. J. Steemers, W. Verboom, D. N. Reinhoudt, E. B. Vander Tol and J. W. Verhoeven, *J. Am. Chem. Soc.*, 1995, **117**, 9408–9414.

15 (a) J. Q. Leng, H. F. Li, P. Chen , W. B. Sun, T. Gao and P. F. Yan, *Dalton Trans.*, 2014, **43**, 12228–12235; (b) F. M. Zhang, P. F. Yan, H. F. Li, X. Y. Zou, G. F. Hou and G. M. Li, *Dalton Trans.*, 2014, **43**, 12574–12581.

16 (a) R. M. Duke, E. B. Veale, F. M. Pfeffer, P. E. Kruger, T. Gunnlaugsson, *Chem. Soc. Rev.*, 2010, **39**, 3936–3953; (b) N. I. Georgiev, A. M. Asiri, A. H. Qusti, K. A. Alamry, V. B. Bojinov, *Sens. Actuators B*, 2014, **190**, 185–198; (c) K. R. Wang, F. Qian, R. X. Rong, Z. R. Cao, X. M. Wang, X. L. Li, *RSC Adv.*, 2014, **4**, 47605–47608; (d) S. Banerjee, E. B. Veale, C. M. Phelan, S. A. Murphy, G. M. Tocci, L. J. Gillespie, D. O. Frimannsson, J. M. Kelly and T. Gunnlaugsson, *Chem. Soc. Rev.*, 2013, **42**, 1601–1618; (e) J. J. Liu, Y. Wang, G. D. Lei, J. B. Peng, Y. Huang, Y. Cao, M. G. Xie, X. M. Pu, Z. Y. Lu, *J. Mater. Chem.*, 2009, **19**, 7753–7758.

17 (a) M. Kleinerman, *J. Chem. Phys.*, 1969, **51**, 2370–2381; (b) J. Andres and A.-S. Chauvin, *Phys. Chem. Chem. Phys.*, 2013, **15**, 15981–15994.

18 (a) B. Ventura, A. Bertocco, D. Braga, L. Catalano, S. d'Agostino, F. Grepioni, P. Taddei, *J. Phys. Chem. C*, 2014, **118**, 18646–18658; (b) S. Mukherjee and P. Thilagar, *Chem. Eur. J.*, 2014, **20**, 9052–9062.

19 T. Smith and J. Guild, *Trans. Opt. Soc.*, 1931, **33**, 73.

20 W. H. Melhuish, *J. Phys. Chem.*, 1961, **65**, 229–235.

21 (a) M. S. Wang, G. C. Guo, W. T. Chen, G. Xu, W. W. Zhou, K. J. Wu and J. S. Huang, *Angew. Chem. Int. Ed.*, 2007, **46**, 3909–3911; (b) M. S. Wang, S. P. Guo, Y. Li, L. Z. Cai, J. P. Zou, G. Xu, W. W. Zhou, F. K. Zheng and G. C. Guo, *J. Am. Chem. Soc.*, 2009, **131**, 13572–13573; (c) A. C. Wibowo, S. A. Vaughn, M. D. Smith, H.-C. zur Loye, *Inorg. Chem.*, 2010, **49**, 11001–11008; (d) J. He, M. Zeller, A. D. Hunter and Z. Xu, *J. Am. Chem. Soc.*, 2012, **134**, 1553–1559; (f) M. Roushan, X. Zhang and J. Li, *Angew. Chem. Int. Ed.*, 2012, **51**, 436–439.

22 (a) L. M. Fu, X. C. Ai, M. Y. Li, X. F. Wen, R. Hao, Y. S. Wu, Y. Wang and J. P. Zhang, *J. Phys. Chem. A*, 2010, **114**, 4494–4500; (b) J. H. Ryu, Y. K. Eom, J.-C. G. Bünzli and H. K. Kim, *New J. Chem.*, 2012, **36**, 723–731; (c) W. K. Lo, W. K. Wong, W. Y. Wong, J. P. Guo, K. T. Yeung, Y. K. Cheng, X. P. Yang and R. A. Jones, *Inorg. Chem.*, 2006, **45**, 9315–9325; (d) P. P. Lima, S. S. Nobre, R. O. Freire, S. A. Júnior, R. A. Sá Ferreira, U. Pischel, O. L. Malta and L. D. Carlos, *J. Phys. Chem. C*, 2007, **111**, 17627–17634.

23 (a) G. F. de Sá, O. L. Malta, C. de Mello Donegá, A. M. Simas, R. L. Longo, P. A. Santa-Cruz and E. F. da Silva Jr, *Coord. Chem. Rev.*, 2000, **196**, 165–195; (b) F. R. Gonçalves e Silva, O. L. Malta, C. Reinhard, H.-U. Güdel, C. Piguet, J. E. Moser and J.-C. G. Bünzli, *J. Phys. Chem. A*, 2002, **106**, 1670–1677.